Angular Distributions of 4.43-Mev Gamma Radiation from $C^{12}(p,p'\gamma)C^{12}$†*

H. S. Adams, J. D. Fox, N. P. Heydenburg,‡ and G. M. Temmer‡
Department of Physics, Florida State University, Tallahassee, Florida

(Received August 7, 1961)

The yield at 90 degrees, and 32 angular distributions of the 4.43-Mev gamma ray from the first-excited state of C^{12} have been measured for proton bombarding energies between 5 and 12 Mev. The excitation curve for inelastic scattering is characterized by a number of strong resonances, some of which were previously known. In addition, underlying the resonances, there is a monotonically rising background. The angular distributions were fitted by least squares to the expression $W(\theta)=A_0+A_2P_2(\cos\theta)+A_4P_4(\cos\theta)$. Those obtained in the region of the resonances at $E_p=5.36$ Mev and $E_p=5.89$ Mev can be interpreted by taking into account these two resonances with respective characters $\frac{3}{2}^+$ and $\frac{5}{2}^+$ plus one additional state at an excitation energy of 6.38 Mev ($\frac{5}{2}^+$) in the compound nucleus N^{13} which can be seen only in elastic scattering. A simple direct-reaction model using a nucleon-nucleon interaction accounts very well for four angular distributions at higher energies in regions showing no resonant structure.

I. INTRODUCTION

THE excitation of the first-excited state of C^{12} at 4.43-Mev and subsequent gamma decay has been studied by inelastic scattering of protons with energies below 20 Mev by a number of groups.[1–4] The precisely controlled energies which have become available with the advent of tandem electrostatic accelerators have led us to investigate the yield and angular distributions of the 4.43-Mev gamma radiation in the proton-energy range between 5 and 12 Mev.

Our program was to measure the yield of gamma radiation at 90° to the beam, as a function of bombarding energy, and then to determine angular distributions at salient points of the excitation curve; some 32 angular distributions were obtained and analyzed near resonances, as well as far from pronounced resonant structure, in an attempt to explore the relative contributions of compound-nucleus formation and direct reaction mechanism. As we shall see, some success in a theoretical understanding of these distributions has been achieved.[5,6]

II. EXPERIMENTAL

The proton beam from our tanden Van de Graaff generator was focused to a 2-mm diameter spot on a thin (~10 kev), self-supporting carbon target, located at the center of a 6-in. diameter cylindrical aluminum chamber with $\frac{1}{2}$-in. wall thickness. After traversing the target, the beam was allowed to continue *in vacuo* for about 7 ft, and was stopped in a piece of lead. Layers of concrete, lead, and paraffin shielded the detector from the beam stopper. The last portion of the beam tube was insulated and served as Faraday cup.

The movable detector was a 5-in. diameter, 4-in. thick NaI(Tl) crystal located on a rotatable arm at about 90 cm from the target, surrounded by a 2-in. lead shield. Angular distribution data were obtained in steps of 15°, usually between 15° and 90°. On several occasions we extended the measurements to the backward hemisphere to check on the required symmetry about 90°; no significant departures were observed.

As an additional check on the centering of the turntable, we placed a Pu-Be neutron source at the target position; this source emits the same 4.43-Mev γ ray isotropically, and we found the gamma-ray counting rate to be constant to within 2%.

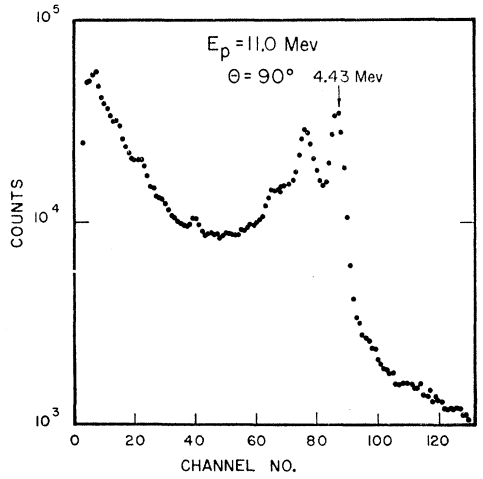

FIG. 1. Typical pulse-height distribution of 4.43-Mev gamma ray observed with 5-in. diameter, 4-in. thick NaI(Tl) crystal 90 cm from carbon target bombarded by 11-Mev protons. Logarithm of counting rate per channel vs channel number. Angular distributions obtained by straddling the single-escape peak (first peak to the left of 4.43-Mev peak) with a single-channel analyzer.

† Supported in part by the Air Force Office of Scientific Research of the Air Force Office of Aerospace Research.

* A preliminary account of this work was presented at the 1960 Thanksgiving meeting of the American Physical Society [Bull. Am. Phys. Soc. **5**, 404 (1960)].

‡ Also Department of Terrestrial Magnetism, Carnegie Institution of Washington, Washington, D. C.

[1] M. Martin, H. Schneider, and M. Sempert, Helv. Phys. Acta **26**, 595 (1953).

[2] C. W. Reich, G. C. Phillips, and J. L. Russell, Jr., Phys. Rev. **104**, 143 (1956).

[2a] H. E. Gove and N. S. Wall, Can. J. Phys. **31**, 189 (1953).

[3] L. J. Lidofsky, J. Weil, R. D. Bent, and K. W. Jones, Bull. Am. Phys. Soc. **2**, 29 (1957).

[4] N. M. Nikolić, L. J. Lidofsky, and T. H. Kruse, Bull. Am. Phys. Soc. **6**, 25 (1961).

[5] M. Nomoto, Air Force Office of Scientific Research Tech. Rept. No. 784, 1961 (unpublished); also Nuclear Phys. (to be published).

[6] M. Nomoto, Air Force Office of Scientific Research Tech. Rept. No. 971, 1961 (unpublished); also Phys. Rev. (to be published).

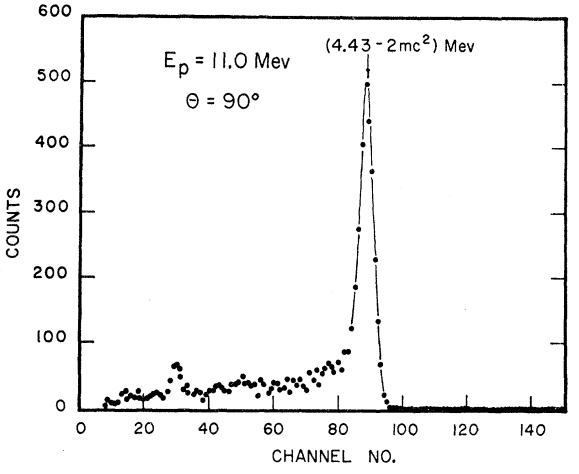

FIG. 2. Typical pulse-height spectrum of 4.43-Mev gamma ray observed with a three-crystal pair spectrometer (a 1½-in.×3-in. crystal flanked by two 3-in.×3-in. crystals) when bombarding a carbon target with 11-Mev protons. Counting rate per channel vs channel number. Peak corresponds to double escape (3.41 Mev). Note complete absence of higher energy gamma radiation.

During the angular distribution measurements, the gamma radiation was monitored by a fixed, 3 in.×3 in. NaI(Tl) scintillation counter located at about 90° to the beam.

A typical pulse-height spectrum of the 4.43-Mev gamma ray in the movable detector is shown in Fig. 1. Figure 2 shows a three-crystal pair-spectrometer spectrum of the same radiation obtained at 11.0-Mev bombarding energy which shows the purity of the gamma spectrum. The spectra in both gamma counters were continuously monitored on a TMC 256-channel analyzer for possible changes in over-all gain, and slight adjustments in the photomultiplier voltages were made to keep the full energy gamma-ray peaks stationary to within one channel. A single pulse-height channel straddling the single-escape peak (E_γ−0.511 Mev) was actually used to measure the relative counting rates in both the movable and fixed detectors. The background rate without target was found to be negligible; in fact, no difference in background was observed whether the beam was intercepted on a tantalum shutter in the main accelerator room, or by the beam stopper beyond the target.

Beam currents of the order of 0.2 μamp were used. All pertinent information for the angular distribution measurements such as magnet frequency (beam energy), angle, monitor count, and movable detector count was automatically recorded on cards by a model 026 IBM card punch for later analysis.

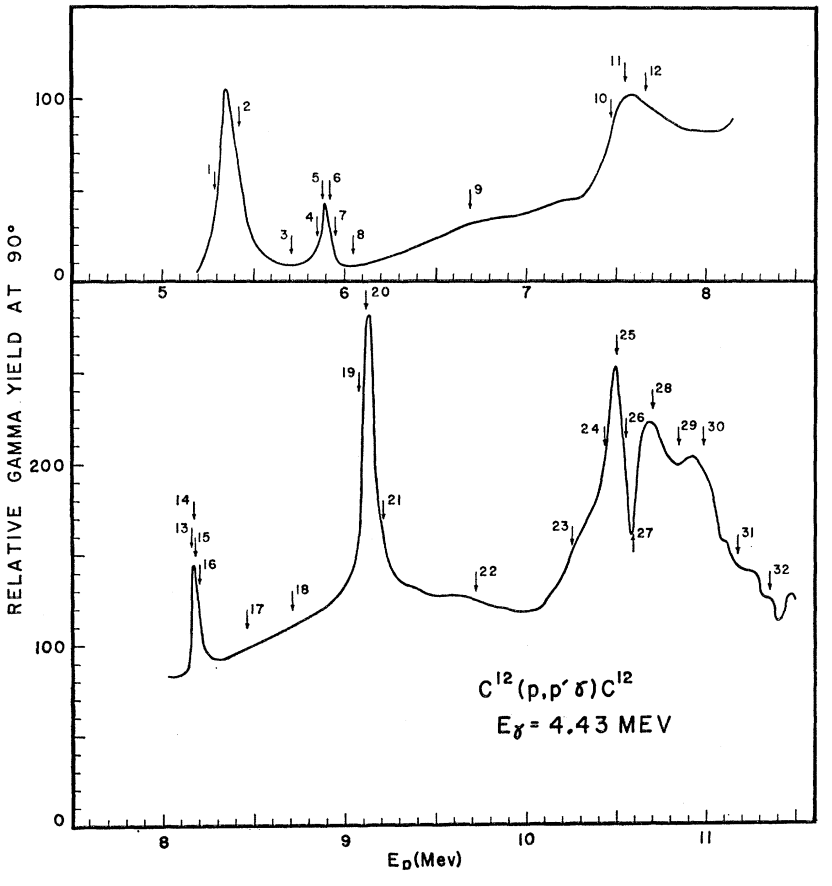

FIG. 3. Excitation curve for 4.43-Mev gamma radiation from the reaction $C^{12}(p,p'\gamma)C^{12}$ between 5.2-Mev and 11.5-Mev proton energy, at 90° to the beam. Numbered arrows indicate energies at which angular distributions were obtained. Numbers agree with those of Fig. 4 and Table I.

III. RESULTS

Figure 3 shows the excitation curve for the yield of gamma radiation at 90° between 5.2-Mev and 11.5-Mev proton bombarding energy. Yields were measured at least every 50 kev, with finer steps whenever indicated. The uncertainties due to counting statistics were kept in the neighborhood of 1%. The numbered arrows in Fig. 3 indicate the energies at which complete angular distributions of the gamma radiation were obtained.

Since the gamma ray represents a pure $E2$ transition (2^+ to 0^+), its angular distribution contains even powers of $\cos\theta$, only up to the fourth:

$$W(\theta)=A_0+A_2P_2(\cos\theta)+A_4P_4(\cos\theta).$$

Two parameters can be extracted from each angular distribution, namely, the quantities A_2/A_0 and A_4/A_0, which contain all information obtainable from such measurements. The values of these coefficients are governed by the properties of the state or states excited in the compound nucleus N^{13}, as well as by the incoming and outgoing proton orbital angular momenta. In the direct-reaction picture, the form assumed for the nucleon-nucleon interaction or nucleon-surface interaction will determine the coefficients.

Values of these coefficients with their least-square uncertainties were extracted from the data with the aid of an IBM 650 computer. They are tabulated in Table I. The uncertainties in both coefficients are seen to lie below 5% in all cases, and are generally considerably smaller. No correction for finite solid angle of the detector was made in view of its smallness. Figure 4 shows the first 10 of the experimental angular distributions and the curves obtained by least-squares fit; they are numbered so as to correspond to the arrows in Fig. 3.

TABLE I. Result of least-squares analysis of gamma-ray angular distribution data. Numbers in first column correspond to arrows in Fig. 3. $W(\theta)=A_0+A_2P_2(\cos\theta)+A_4P_4(\cos\theta)$.

No.	E (Mev)	A_2/A_0	A_4/A_0
1	5.29	0.442±0.018	0.154±0.027
2	5.42	0.648±0.026	−0.442±0.037
3	5.71	0.616±0.012	−0.902±0.018
4	5.85	0.551±0.007	−0.623±0.011
5	5.88	0.532±0.005	−0.574±0.007
6	5.92	0.563±0.009	−0.774±0.013
7	5.95	0.595±0.012	−0.962±0.017
8	6.05	0.502±0.017	−0.998±0.024
9	6.69	0.213±0.014	−0.336±0.019
10	7.47	0.269±0.011	−0.442±0.016
11	7.55	0.218±0.014	−0.496±0.021
12	7.66	0.287±0.014	−0.414±0.020
13	8.16	0.335±0.010	−0.285±0.015
14	8.17	0.374±0.013	−0.241±0.019
15	8.18	0.395±0.009	−0.269±0.013
16	8.20	0.395±0.007	−0.391±0.010
17	8.46	0.358±0.019	−0.440±0.027
18	8.71	0.326±0.013	−0.387±0.020
19	9.08	0.168±0.010	−0.271±0.013
20	9.12	0.166±0.009	−0.156±0.015
21	9.21	0.230±0.018	−0.153±0.019
22	9.72	0.177±0.010	−0.223±0.017
23	10.25	0.303±0.007	−0.446±0.010
24	10.43	0.161±0.009	−0.163±0.012
25	10.50	0.074±0.010	−0.051±0.016
26	10.55	0.072±0.009	0.031±0.014
27	10.59	0.103±0.009	0.199±0.014
28	10.70	0.194±0.006	0.247±0.010
29	10.84	0.265±0.011	−0.136±0.016
30	10.98	0.333±0.005	−0.357±0.007
31	11.17	0.336±0.005	−0.384±0.008
32	11.35	0.357±0.011	−0.385±0.017

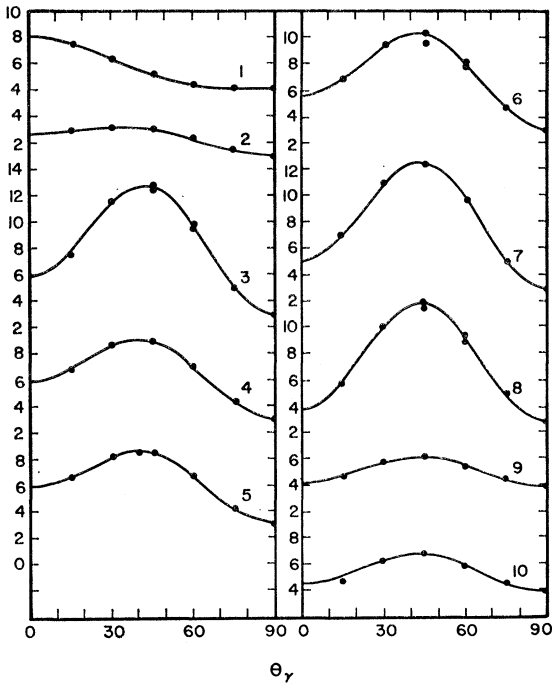

FIG. 4. Angular distributions of 4.43-Mev gamma radiation from $C^{12}(p,p'\gamma)C^{12}$. Numbers refer to arrows of Fig. 3 (bombarding energies) and identify the distributions in Table I. Solid points are experimental points; curves represent least-squares fits whose parameters are to be found in Table I. Curves are symmetric about 90°.

1. Bombarding Energy below 6 Mev

The pronounced resonances between 5 and 6 Mev have received some attention previously. Two strong gamma-ray resonances were reported by Swiss workers[1] at 5.37 and 5.9 Mev, using a cyclotron. Reich *et al.*[2] have examined elastic scattering angular distributions as well as the gamma-ray angular distributions at energies up to 5.7 Mev. These authors assigned a $\frac{3}{2}^+$ character to the state at 5.36-Mev bombarding energy (6.91-Mev excitation in N^{13}) and inferred the possibility of another interfering level of character $\frac{5}{2}^+$ in the vicinity. This is clearly apparent, since a pure $\frac{3}{2}^+$ resonance would yield angular distributions with $A_4=0$. A glance at Table I reveals nonzero fourth-order coefficients on either side of the peak of the resonance (distributions Nos. 1 and 2) but of opposite sign. The interfering level must have a spin of at least $\frac{5}{2}$, and the orbital angular momentum of the incoming protons must be at least 2. Angular distributions No. 4, 5, 6,

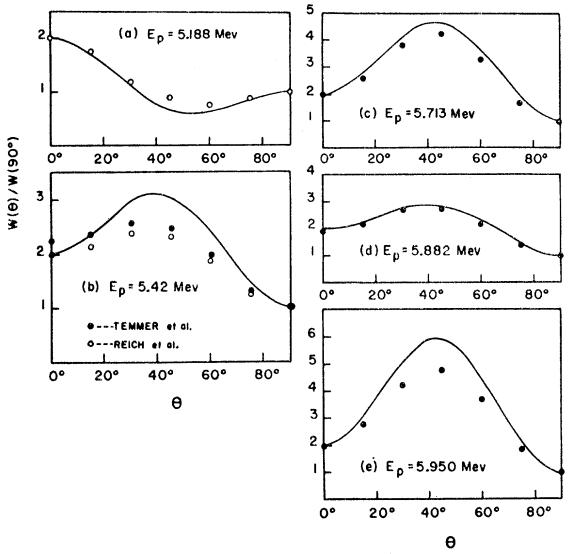

FIG. 5. Angular distributions of 4.43-Mev gamma radiation from $C^{12}(p,p'\gamma)C^{12}$. All solid curves are theoretical interpretations in terms of three resonances as obtained by Nomoto[5] and are normalized to unity and to the experimental points at 90°. Open circles give experimental data of Reich *et al.*[2]; solid dots are our data. Curves (b), (c), (d), and (e) correspond to No. 2, 3, 5, and 7, respectively, of Figs. 3 and 4, and Table I.

and 7 (Table I and Fig. 4) on the resonance at 5.89 Mev (7.42-Mev excitation in N^{13}) have shapes most nearly like distributions for a $\frac{5}{2}^+$ state excited by $l=2$ protons, with outgoing protons having $l'=0$ and outgoing channel spin $s'=\frac{5}{2}$, but with significant departures from that shape. Nomoto[5] has attempted to fit these four angular distributions in terms of the interference of the two resonances at 5.36 and 5.89 Mev, leaving the ratio of their reduced widths as an adjustable parameter. No consistent fit was obtainable, and he concluded that at least one additional compound state was contributing in this region. A $\frac{5}{2}^+$ state previously identified by elastic scattering at 6.38-Mev excitation in N^{13},[2] although unobservable by inelastic scattering for energetic reasons, can nevertheless influence the angular distributions, as shown by Nomoto's analysis.[5] He analyzed some of our angular distributions in this region (No. 2, 3, 5, and 7 of Table I and Fig. 4) by taking into account the three resonances at excitation energies of 6.38 Mev ($\frac{5}{2}^+$), 6.91 Mev ($\frac{3}{2}^+$), and 7.42 Mev ($\frac{5}{2}^+$). There were two free parameters in the problem, namely, the two independent ratios of the "reduced widths"[7] of the three states in question. Figure 5 shows the results of these theoretical fits to some of our angular distributions, as well as some previously obtained by Reich *et al.*[2] The agreement is seen to be fairly good, but the experimental angular distributions are found to be less pronounced in all cases. Subsequent to this work, Nikolić *et al.*[4] reported evidence for a weak state of spin $\frac{1}{2}^\pm$, located at 5.68-Mev bombarding energy (7.20-Mev excitation in N^{13}). Our excitation curve is consistent with the existence of this weak state. Such a state, if included in the analysis, would contribute an isotropic component to the angular distribution, and hence bring experiment and theory into closer agreement.[8]

In addition, there is evidence for a very broad state at about 6.7-Mev bombarding energy,[9] and possibly others that may affect the angular distributions in this energy region. No further analysis in terms of several contributing compound resonances was attempted. Analysis of elastic and inelastic scattering data[10,11] may shed some more light on this situation.

It is clear that even at our lowest excitation energies we are faced with a rather complex situation: The excitation function is still dominated by strong resonances, but their widths, strengths, and spacings are such that a number of them have to be taken into consideration at any given bombarding energy. A simplified picture which profits from assuming very high level densities does not seem appropriate at this point. Table II summarizes the resonances we observe, and their approximate widths.

2. Bombarding Energy above 6 Mev

Beyond 6-Mev bombarding energy, the most striking feature in the excitation curve is the more or less monotonically increasing yield which underlies all structure at the higher energies. It is tempting to associate this yield with some type of direct reaction. Nomoto[6] has investigated the angular distributions to be expected when assuming a direct nucleon-nucleon interaction potential localized in the nuclear surface, and consisting of a spin-flip part plus a non-spin-flip part. He used $j-j$ coupling shell-model wave functions for the ground

TABLE II. Prominent resonances observed in the reaction $C^{12}(p,p'\gamma)C^{12}$. E_{res} = resonant proton bombarding energy; E^* = excitation energy in N^{13}; Γ_{lab} = full width at half-maximum in the laboratory.

E_{res} (Mev)	E^* (Mev)	Γ_{lab} (kev)
5.36[a]	6.89	140
5.89[a]	7.38	70
7.55	8.91	255
8.17	9.98	38
9.12	10.36	70
10.51	11.64	85
10.74	11.85	140
10.99	12.09	150

[a] Previously observed (see reference 2).

[7] Each of these "reduced widths" are actually products of square roots of incoming and outgoing proton reduced widths.

[8] This does not include the *interference* effect for a $\frac{1}{2}^+$ state which may contain a term in $P_2(\cos\theta)$ when interfering with $\frac{3}{2}^+$ and $\frac{5}{2}^+$ states, but only for outgoing proton angular momentum $l'=2$, which is expected to be small compared to the favored $l'=0$ contribution. If the state is $\frac{1}{2}^-$, the interference term vanishes and we only have the isotropic admixture mentioned above.

[9] H. Schneider, Helv. Phys. Acta **29**, 55 (1956).

[10] F. L. Bordell, G. E. Mitchell, P. B. Weiss, J. W. Nelson, and R. H. Davis, Bull. Am. Phys. Soc. **5**, 404 (1960), and private communication.

[11] V. R. McKenna, A. M. Baxter, and G. G. Shute, Australian J. Phys. **14**, 196 (1961).

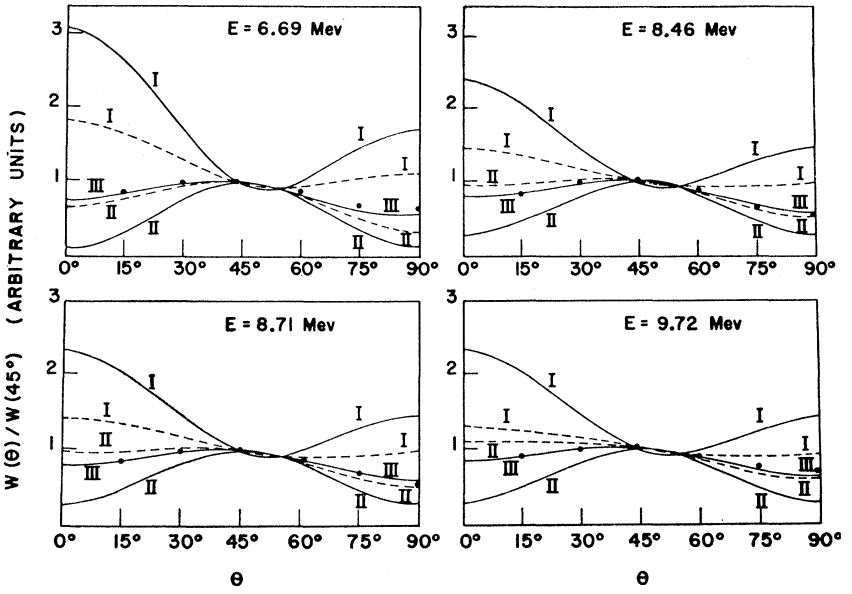

FIG. 6. Angular distributions of 4.43-Mev gamma radiation from $C^{12}(p,p'\gamma)C^{12}$. Solid dots represent our experimental data. Bombarding proton energies of 6.69, 8.46, 8.71, and 9.72 Mev correspond to No. 9, 17, 18, and 22, respectively, as defined in Figs. 3 and 4, and Table I. All curves are theoretical as obtained by Nomoto from a direct-reaction picture,[6] and are normalized to the data at 45°. Dashed curves (I) and (II) correspond to plane-wave approximation, spin-flip ($a_1=1$, $a_0=0$) and non-spin-flip ($a_1=0$, $a_0=1$) interaction potential, respectively; solid curves (I) and (II) correspond to distorted-wave calculation, spin-flip, and non-spin-flip potential, respectively. Solid curves (III) represent the best fit: distorted waves and $|a_1/a_0|=0.67$.

and first-excited states of C^{12}, as indicated by the calculations of Glendenning,[12] and Levinson and Banerjee.[13] Figure 6 shows a comparison of Nomoto's theoretical curves and our data corresponding to distributions No. 9, 17, 18, and 22 of Table I and Fig. 3. At these bombarding energies the excitation curve is seen to be smooth and reasonably free of pronounced resonant structure. Remarkably good agreement with the four experimental curves is obtained for the same mixture[14] of non-spin-flip and spin-flip interaction. Furthermore, the experimental curves fall outside of the extremes allowed by plane-wave Born approximation, and hence definitely require the consideration of distortion effects.

We have not attempted to interpret angular distributions above 10 Mev. A very wide and complex structure can be seen in the excitation curve between 10 and 11.5 Mev (cf. Fig. 3), consisting of at least 6 resonances, and possibly more.[10] These are superimposed on a background which we believe to be due to some form of direct process, as corroborated by agreement with the theoretical analysis.[6] In view of the relative complexity in dealing with just three resonances[5] (see above), an extension of this approach including more resonances does not seem fruitful.

The peaks in the excitation curve at 7.55, 8.17, and 9.12 Mev proton energy are probably due to single compound states. In view of the sucessful interpretation of our angular distributions in the comparatively uneventful regions between these resonances in terms of a simple direct reaction picture, it may be possible to interpret the angular distributions on these resonances by combining the amplitude of a single resonance (once its spin and parity are known) with the direct-reaction amplitude. This possibility is presently under investigation.

[12] N. K. Glendenning, Phys. Rev. **114**, 1297 (1959).

[13] C. A. Levinson and M. K. Banerjee, Ann. Phys. **2**, 471 (1957); *ibid.* **2**, 499 (1957); *ibid.* **3**, 67 (1958).

[14] This mixture is given by $a_0/a_1=\pm 0.67$, where a_0 measures the non-spin-flip portion, and a_1 the spin-flip portion of the interaction potential (see reference 6). These proportions are close to the so-called Rosenfeld mixture if the minus sign applies. [L. Rosenfeld, *Nuclear Forces* (North-Holland Publishing Company, Amsterdam, 1948), Chapter 11.]

ACKNOWLEDGMENTS

We have enjoyed useful discussions with Dr. M. Nomoto on the interpretation of our results. We also wish to thank J. A. Becker and H. R. Blieden for their assistance during the measurements.